IRIS AperTO

UNIVERSITÀ DEGLI STUDI DI TORINO

AperTO - Archivio Istituzionale Open Access dell'Università di Torino

Cationic liposomal vectors incorporating a bolaamphiphile for oligonucleotide antimicrobials

This is a pre print version of the following article:

Original Citation:

Availability:

This version is available http://hdl.handle.net/2318/1896672 since 2023-03-23T14:05:54Z

Published version:

DOI:10.1016/j.bbamem.2017.06.006

Terms of use:

Open Access

Anyone can freely access the full text of works made available as "Open Access". Works made available under a Creative Commons license can be used according to the terms and conditions of said license. Use of all other works requires consent of the right holder (author or publisher) if not exempted from copyright protection by the applicable law.

(Article begins on next page)

02 May 2024

Cationic liposomal vectors incorporating a bolaamphiphile for oligonucleotide antimicrobials

Marianna Mamusa [a,*], Leopoldo Sitia [b], Francesco Barbero [c], Angels Ruyra [d], Teresa Díaz Calvo [b], Costanza Montis [a], Ana Gonzalez-Paredes [c], Grant N.Wheeler [d], Christopher J. Morris [e], Michael McArthur [b,f], Debora Berti [a]

a Department of Chemistry "Ugo Schiff" and CSGI, University of Florence. Via della Lastruccia 3, 50019 Sesto Fiorentino, (FI), Italy
b Procarta Biosystems Ltd, Norwich Research Park, Norwich NR4 7UH, United Kingdom
c Nanovector s.r.l., Via Livorno 60, 10144 Torino, Italy
d School of Biological Sciences, University of East Anglia, Norwich Research Park, Norwich NR4 7TJ, United Kingdom
e School of Pharmacy, University of East Anglia, Norwich Research Park, Norwich NR4 7TJ, United Kingdom
f Norwich Medical School, University of East Anglia, Norwich Research Park, Norwich NR4 7UQ, United Kingdom

ABSTRACT

Antibacterial resistance has become a serious crisis for world health over the last few decades, so that new therapeutic approaches are strongly needed to face the threat of resistant infections. Transcription factor decoys (TFD) are a promising new class of antimicrobial oligonucleotides with proven in vivo activity when combined with a bolaamphiphilic cationic molecule, 12-bis-THA. These two molecular species form stable nanoplexes which, however, present very scarce colloidal stability in physiological media, which poses the challenge of drug formulation and delivery. In this work, we reformulated the 12-bis-THA/TFD nanoplexes in a liposomal carrier, which retains the ability to protect the oligonucleotide therapeutic from degradation and deliver it across the bacterial cell wall. We performed a physical-chemical study to investigate how the incorporation of 12-bis-THAand TFD affects the structure of POPC- and POPC/DOPE liposomes. Analysis was performed using dynamic light scattering (DLS), ζ-potential measurements, small-angle x-ray scattering (SAXS), and steady-state fluorescence spectroscopy to better understand the structure of the liposomal formulations containing the 12-bis-THA/TFD complexes. Oligonucleotide delivery to model Escherichia coli bacteria was assessed by means of confocal scanning laser microscopy (CLSM), evidencing the requirement of a fusogenic helper lipid for transfection. Preliminary biological assessments suggested the necessity of further development by modulation of 12-bis-THA concentration in order to optimize its therapeutic index, i.e. the ratio of antibacterial activity to the observed cytotoxicity. In summary, POPC/DOPE/12-bis-THA liposomes appear as promising formulations for TFD delivery.

INTRODUCTION

The emergence of drug-resistant microbial strains is a natural phenomenon that occurswhen bacteria evolve and adapt to face the threats posed by antimicrobial agents [1].However, this process has been greatly accelerated by the excessive and incorrect use of antibacterial drugs. This has resulted in the lack of available treatments for once curable infectious diseases [2,3], determining a world-wide health crisis as reported by the World Health Organization [4]. In this context, renewed interest by public and private initiatives has focused on innovative approaches [5]. Among several alternative approaches proposed [6–11], transcription factor decoys (TFD) have shown the potential to defeat resistant infections, such as those caused by Clostridium difficile in animal models [12], when combined with a bolaamphiphilic cationic delivery molecule (12-bis-THA) to form nanosized association complexes, termed nanoplexes. TFDs are short oligonucleotides consisting of base sequences that mimic the binding site to transcription factors, and they can block essential genetic pathways in bacteria, thereby preventing their survival response against antimicrobial attack [13]. The cationic surfactant 12-bis-THA is a bolaamphiphile with a molecular structure reminiscent of dequalinium,which is prescribed as a topical treatment for various bacterial infections. Besides its intrinsic antibacterial activity, owing to the positive electrostatic charge, dequaliniumhas been studied as a scaffold for gene delivery systems [14]. Similarly, 12-bis-THA plays a fundamental role in forming nanoplexes with oligonucleotides, which are condensed into a psi-form [15]: this structural rearrangement affords both resistance to DNA degradation [16] and DNA delivery into live cells [17]. The condensation process is reversible, as the fully renatured oligonucleotide can be released from the complex with 12-bis-THA by displacing it with a competing anionic molecule [15]. 12-bis-THA/TFD nanoplexes have been shown to be active in animal studies [17], but it is known that their colloidal stability needs to be improved prior to preclinical development, as they have the tendency to forminsoluble precipitates in conditions of physiological ionic strength. The optimized delivery system would also have controllable physicalchemical properties, as these affect the biodistribution of the nanoplexes and thus which infections can be treated. All of these requirements can be met by liposomes (or small unilamellar vesicles, SUV): these can be formulated from biocompatible lipids, and they have been successfully used as drug carriers [18] and transfection vectors [19]. In particular, several antibiotics already commercially distributed are formulated on a liposomal scaffold [20], and liposomes have been proposed as antisense DNA vectors to bacteria [21]. In the present work, we redesigned the 12-bis-THA/TFD antimicrobial complex in a stable liposomal formulation that can retain delivery to the bacterial cytoplasm. Given the amphiphilic nature of 12-bis-THA, the encapsulation of nanoplexes in liposomes poses some challenges. A physical-chemical study was therefore necessary to assess the possible influence of the payload on liposomal stability and bilayer integrity [22,23]. Therefore, we first investigated the effect of 12-bis-THA on the structure of liposomes based on classic lipids, i.e. neat POPC or a POPC/DOPE mixture; next, the formulations were investigated in-depth to elucidate the nanoscale features of the bilayer, focusing in particular on the POPC/DOPE scaffolds. A preliminary biological evaluation was carried out to assess the transfection ability to model bacteria, the antibacterial activity and the cytotoxicity of these promising formulations.

RESULTS AND DISCUSSION

We recently showed, using a range of complementary physical techniques, that 12-bis-THA (Scheme 1) complexes TFDs into a highly compacted, nuclease-resistant "psi" form in aqueous solution [15]. Here we studied the kinetics of nanoplex stability by dynamic light scattering (DLS), monitoring the variation of hydrodynamic diameter (DH) and average scattered intensity (Iav) in water and in saline media at physiological ionic strength. As illustrated in Fig. 1A, nanoplexes in H2O stored at 4 °C were stable for at least 72 h in terms of size. The stability of particles in water at RT (Fig. 1B)was limited to 24 h,when they were observed to become slightly larger; in seven days, the size had increased by almost 100% while the scattering intensity was reduced by 7.5 times (data not shown). Indeed, since the light scattered by colloidal objects in solution is proportional to their concentration, such a dramatic decline of Iav clearly indicates the steep decrease of the number of suspended particles in solution as they progressively precipitate. The few particles remaining in suspension became larger over time due to coalescence and would most likely precipitate in time. Near instantaneous aggregation was observed after incubating the nanoplexes in saline solutions with physiological ionic strength (sodium citrate orsodium chloride, 150 mM). This phenomenon is expected, due to the electrostatic origin of colloidal stability in water. The screening of the electrostatic charge of ionic colloids in the presence of dissolved salts, according to the DLVO theory of colloidal stability, triggers aggregation and eventually precipitation [28]. At the same time, this denotes the marked instability of the 12-bis-THA/TFD antibacterial complex in saline media. In light of these results, we resorted to the reformulation of the 12-bis-THA/TFD nanoplexes in a lipid-based scaffold. Liposomes for drug delivery are typically obtained with biocompatible lipids. We report here on the incorporation of 12-bis-THA and the loading of a model TFD in two lipid systems: one based on pure POPC and another based on the mixture of POPC and DOPE (1,2-dioleoyl-snglycero-3-phosphoethanolamine) in a 7:3 weight ratio. DOPE has been used for a long time as a helper lipid to promote fusion of liposomes with biological membranes, with proven ability to boost DNA transfection [29] and antibiotic efficacy [30]. The symmetric bolaamphiphile 12-bis-THA is poorly soluble in water and does not behave like a typical surfactant, as it has no clearcut critical micellar concentration [15]. However, the presence of two cationic headgroups along with a 12-C aliphatic chain spacer suggests the possibility of amphiphilic behaviour. In order to assess the effect of the bolaamphiphile on the integrity of lipid bilayers, we firstly incorporated 12-bis-THA into liposomes following two different paths. In the "co-extrusion method", 12-bis-THA (0.2 mM) was mixed with other lipids (5mg/mL) in the initial dry film before hydration and membrane extrusion. In the "surface decoration method", pre-extruded liposomes were added to a dry film of 12-bis-THA to allow the uptake of the bolaamphiphile into the bilayers. The two protocols are represented in Scheme 2.

The physical-chemical characterization of such liposomes is given in Table 1. For both POPC- and POPC/DOPE systems, the initial negative ζ-potentials of pure liposomes reversed upon introduction of 12-bis-THA, confirming the binding of the bolaamphiphile to liposomes with both methods. The co-extrusion protocol originated smaller POPC- and POPC/DOPE liposomes than the decoration method, suggesting that in the former 12-bis-THA partitions between the inner and outer leaflet of the bilayer, while in the latter the bolaamphiphile accumulates at the liposomal surface. Importantly, the ζ-potentials of the vesicles decorated with 12-bis-THA remained constant around the value +25 mV (within the error bar; data not shown) even after an 80-fold dilution, demonstrating that the bolaamphiphile is strongly associated with the bilayer and does not desorb upon dilution. Although the hydrodynamic size increased, 12-bis-THA did not change the morphology of liposomes, as demonstrated in a cryo-TEM image (Fig. S1, Supporting Information) showing spherical liposomes made of POPC and 12-bis-THA introduced by surface decoration. Most importantly, POPC- and POPC/DOPE liposomes containing 12-bis-THA did not show any precipitation or other signs of

colloidal instability when diluted 1:10 and 1:20 with high ionic strength media such as LB broth NaCl 150 mM solution (data not shown), contrary to the neat 12-bis-THA/TFD nanoplexes. However, HPLC analysis of the liposomal dispersions obtained by co-extrusion revealed that approximately 50% of the 12-bis-THAwas incorporated into the final liposome suspension (data not shown). Similarly, we encountered a loss of oligonucleotide when loading a model TFD (12-bis-THA/TFD charge ratio Z+/− = 22) into the liposomes using the co-extrusion protocol. Indeed, the extrusion process was extremely slow and difficult, suggesting rapid adsorption ofmaterial on the polycarbonate membrane. The TFD content in the extruded formulation was assessed by staining with the DNA-binding fluorescent probe OliGreen®, and compared to the TFD content of the dispersion of multilamellar vesicles (MLV) before extrusion (see Fig. S2, Supporting Information). The assay yielded 84% (±10%) of the theoretical TFD amount in the MLV dispersion after disruption of the membranes with Triton X-100, while in the extruded liposomes no DNA could be detected. This suggests that all the TFD was lost during the extrusion process. Several hypotheses can be formulated to possibly explain the loss of material described above. Firstly, DSC experiments ruled out the possible increase in the gel-to-fluid transition temperature, Tm, for the lipid bilayers. Indeed, no transition peaks were observed in the 4 °C–80 °C range (data not shown), which suggests that these lipid assemblies should be easily extruded at room temperature. In another possible scenario, the presence of both the TFD and 12-bis-THA in the initial lipid dry film may promote the formation of the strong complex between the two species directly in the hydrated bilayers, producing lipoplexes in a columnar phase, as observed in similar systems [31]. These species are often rigid and larger than 100 nm, with a greater propensity to obstruct the membrane pores, impeding the passage of the dispersion. In order to examine for such liquid-crystalline phases, we carried out a small-angle x-ray (SAXS) investigation of the POPC/DOPEMLV systems, without and with added bolaamphiphile or TFD, before extrusion. As shown in Fig. 2, MLVs of POPC/DOPE without and with TFD (Fig. 2A,B) display the typical pattern of a lamellar phase with Bragg peaks, which occur at Q=2π/d values due to the interaction between adjacent lipid bilayers. From the first Bragg reflection order, we obtained the lamellar repeat spacing d = 62.8 Å for both samples (without and with TFD), indicating that there is no effect of the TFD on the bilayer structure. Further data modelling was performed by treating the structure factor S(Q) according to the Modified Caillé Theory [32], while the total scattering intensity I(Q) was modeled according to Eq. (1):

$$I(Q) = \frac{(1-N_{diff})S(Q)P(Q) + N_{diff}P(Q)}{Q^2}$$

which is a linear combination of the contributions S(Q) and P(Q) (form factor)weighed on the fraction N diff of positionally uncorrelated bilayers (i.e., unilamellar vesicles). The electron density of the lipid bilayer was modelled using three-Gaussian profiles [33]: two Gaussians represent the headgroups, centered at zH, and one Gaussian is used to represent the terminal −CH3 group at the bilayer's center. The procedure allowed us to determine the center zH and the width σH of the Gaussians representing the headgroups, and to calculate the bilayer thickness (i.e. the headgroup-to-headgroup thickness of the lipid double-layer) as:

$$d_B = 2(z_H + 2\sigma_H)$$

The salient structural features of amodel bilayer, alongwith a typicalelectron density profile (ρ(z) as a function of the distance z fromthe bilayer center) are represented in Scheme 3, while fit results for

the patterns in Fig. 2 are displayed in Table 2. For the POPC/DOPE system, we determined dB=51 Åwithout TFD and dB = 52 Å with TFD. Assuming the average headgroup thickness to be the weighted average of the phosphatidylcholine and phosphatidylethanolamine headgroups [34], dH = 8.9 Å, through an elementary geometric deduction (Scheme 1)we obtain for half the hydrophobic region dC ≈ 16 Å. This value is comparable to that reported in the literature for POPC bilayers at 2 °C [35], nevertheless, our calculated dC pertains to samples at 25 °C and is likely due to presence of 30% DOPE in the bilayer. However, care must be taken when dealing with SAXS patternswhere less than four Bragg peaks are present, as the resolution of the electron density profile is low [36] and it is not always possible to discern the exact threshold between headgroup and tail Gaussians. The spectra pertaining to the samples containing also 12-bis-THA, with and without TFD (Fig. 2C,D), are both consistent with the pure form factor P(Q) of non-interacting lipid bilayers, i.e. only unilamellar vesicles are present. These form spontaneously upon incorporation of 12-bis-THA in the bilayer due to the positive charges of the bolaamphiphile molecules [37], as the bilayer bends in order to minimize repulsion between neighbouring headgroups, and the formation of MLVs is hindered by strong electrostatic repulsion between neighbouring bilayers. Interestingly, there is no trace of liquid-crystallinephases in the POPC/DOPE/12-bis-THA/TFD system. Evidently, the 12-bis-THA/TFD charge ratio used in this instance is too high to induce the formation of lipoplexes in columnar liquid-crystalline phases. Therefore, we can hypothesize that the reason for the observed loss of material during MLV extrusion could be the affinity of the 12-bis-THA/ TFD complex for polycarbonate membranes. Indeed, in some experiments 12-bis-THA iodide (which is poorly water soluble; data not shown) has shown a marked tendency to adsorb on polycarbonate filters; the charge-neutralized complex with TFD might possess a similar affinity for the extrusion filters due to hydrophobic interactions. Another possible reason could be an increased permeability of the vesicles due to a detergency effect of 12-bis-THA, although preliminary studies involving the interaction of the bolaamphiphilewith DPPC bilayers (unpublished) have shown that detergency should take place for higher 12-bis-THA concentrations than those used in the present work. Eventually,we tackled this issue by turning to the surface decoration method. POPC- and POPC/DOPE dry films were hydrated with a TFD solution to increase the chance of encapsulating part of the DNA in the liposomal cores. After extrusion, 12-bis-THAwas taken up froma dry film onto the pre-formed liposomes. ζ-potential measurements were positive whenever 12-bis-THA was included, even in the presence of the TFD (positive-to-negative charge ratio $Z+/-$ = 22), and repeated DLS analysis showed no variation in either size, polydispersity index, or scattering intensity of POPC and POPC/DOPE liposomes over at least three months (data not shown), attesting the high colloidal stability of these systems. Dilution of the formulations in saline NaCl 150 mM did not lead to turbidity or precipitation. Therefore, both types of liposomes appear compatible, for size and surface charge as well as for their stability in time, with the desired application as gene delivery vectors. At this point, since the bolaamphiphile is in large excess compared to the oligonucleotide, one could argue that the addition of 12-bis-THA to the preformed liposomes in a TFD solution might lead to the formation of free TFD/12-bis-THA nanoplexes in the bulk solvent (Scheme 4, scenario b). In order to confirm the localization of the TFD at the positively charged liposomal surface (scenario a in Scheme 4), the nanoscale structure of POPC/DOPE/12-bis-THA liposomes containing growing amounts of TFD was investigated by means of synchrotron SAXS. The spectra recorded for the systems with 0, 10, and 20 μg/mL TFD are shown in Fig. 3 along with the respective best model fits obtained with Eq. (1). The spectra are all similar and they show both a structure factor and a form factor. This suggests the presence of residual oligolamellar vesicles (OLV), where the bilayers are in interaction with each other: OLV contribute greatly to the scattered radiation evenwhen they are present in very small numbers. Only two Bragg reflections are observed, due to bilayer disorder originating from bending fluctuation in the fluid Lα

phase (third kind- or Caillé disorder) [36]. For the liposomes with noTFD, the fit results presented in Table 3 indicate that the SAXS pattern is consistent with a maximum number of 2 interacting lamellae; such bi-lamellar vesicles are present in very low number, since the contribution of the diffuse scattering is Ndiff = 97% of the total I(Q). The bilayer thickness calculated with Eq. (2) is dB=48 Å, in agreement with previous results (Table 2). In liposomes with 10 μg/mL TFD, the quality of the fitting was slightly poorer than for the spectrum of neat POPC/DOPE/12-bis- THA liposomes. Here, the number of interacting lamellae was constrained to 2 during the fitting procedure. The bilayer thickness obtained from the electron density profiles was 50 Å, which is 2 Å larger than the value obtained for the sample without TFD. At [TFD]= 20 μg/mL, data modelling with Eq. (1) fails, most probably due to this model being unable to account for bilayer asymmetry. Such asymmetry between outer and inner lipid leaflets is suggested bythe non-zero second node in the experimental scattering pattern [38], and can be explained by considering that the TFD molecules can only interact by charge compensation with the 12-bis-THA adsorbed on the outer liposomal leaflet. With growing TFD concentration, this effect becomes more evident ad more oligonucleotide accumulates at the surface. For this reason the scattering curves for the samples with [TFD] = 0 and 10 μg/mL can still be fitted using the model of Eq. (1), but not the one with [TFD] = 20 μg/mL. This result supports the scenario in which no 12-bis-THA/TFD nanoplexes are formed in the bulk solution. This hypothesis is further reinforced by the fact that, upon dilution of the formulations in salinemedia, no turbidity or precipitation occur (data not shown). Indeed, since the nanoplexes are unstable in such media, as shown in the first part of this work, the absence of precipitate can safely be taken as proof that no free nanoplexes are present in the bulk solution of the liposomal formulations. Liposomes decoratedwith 12-bis-THA were also loaded with a fluorescently (green) labelled TFD and challenged against a standard laboratory E. coli strain, where the bacterial membrane was labelled with a red fluorophore. The samples were imaged by means of confocal laser scanning microscopy (CLSM); at least 10 different fields of view were evaluated, with a total number of analyzed bacteria cells of approximately 5000. The detection limits of our CLSM experiments demanded the incubation of bacterial cellswith relatively high concentrations of liposome suspensions, in the order of 2.65 mmol/L total lipids, corresponding to 90 μM of 12-bis-THA. In the case of the POPC/12-bis-THA/TFD systems, images (Fig. 4a,b) clearly showan interaction with the bacterial membranes,with evident accumulation of green fluorescentmaterial at the poles and the septa of the bacteria. These are the areas of the E. coli membrane especially rich in cardiolipin [39], a doubly-anionic lipid that is also present at high concentrations in the mitochondrial membrane of eukaryotic cells [40]. This result is in agreement with research involving the interaction of 12-bis-THA with model membranes [17] and the use of dequalinium as an efficient targeting system for mitochondria [41]. Moreover, a recent paper has demonstrated the key role of cardiolipin in the binding of cationic antimicrobial peptides and the perturbation of model bacterial membranes [42], which strengthens evenmore the idea that the affinity of certain cationic antimicrobials for cardiolipin could be exploited as an active targeting mechanism. However, the TFD release and delivery efficiency to the E. coli cytoplasm was low for POPC/12-bis-THA/ TFD liposomes, with b2% of the visualized cells presenting a diffuse intracellular green signal compatible with intracellular TFD release. The situation is rather different for POPC/DOPE liposomes: Fig. 4c,d clearly show a diffuse green fluorescence in the bacterial cytoplasm, confirming the effective delivery of the TFD across the E. coli membrane. This hints at the fundamental role of DOPE in promoting the fusion of liposomal bilayers with bacterial membranes, leading to the release of the TFD in the cytoplasm. Therefore, the fusogenic DOPE lipid is a key component for maximized delivery of the TFD nanoplexes to the bacterial cell. A possible explanation may lie in the fact that the E. coli innermembrane is composed of N80% phosphatidylethanolamine lipids [43,44]. Liposomes based on the POPC/DOPEmixture were tested for their biological properties of interest, namely antibacterial activity and toxicity, in vitro and in

vivo. To determine the activity of liposomal formulations on bacterial membranes a standard bacterial growth assay was used against the model Escherichia coli. As reported in Table 4, both POPC/DOPE/12-bis-THA and POPC/DOPE/12-bis-THA/ TFD liposomes showed similar antibacterial activity of 1.1 μmol/L(with reference to 12-bis-THA, see Fig. S3 for corresponding growth curves), which compares with that of the bare nanoplex [17]. Hence, despite the differences seen in the CLSM results concerning the efficacy of delivery for the two formulations (Fig. 4), the membrane activity of the formulations was correlated to the concentration of 12-bis-THA. The cytotoxicity of liposomal formulations was evaluated by measuring IC50 values with the MTT assay on Caco-2 intestinal epithelial cells (Table 4). Liposomes devoid of 12-bis-THA inflicted no measurable cytotoxicity up to a concentration of ~0.5 mM total lipids. For POPC/DOPE/12-bis-THA and POPC/DOPE/12-bis-THA/TFD liposomes the values of IC50 were 34 μM and 32 μM, respectively. The concentration of total lipids at these IC50 concentrations would be consistent with the 20:1 ratio of lipid:12-bis-THA, i.e. 680 and 640 μM, respectively. IC50 values were comparable to the values gained for other transfection agents [45–47] and approximately twofold lower than that recorded for TFD/12-bis-THA nanoplexes [17]. The combination of improved colloidal stability of 12-bis-THA liposome formulations (cf. nanoplexes) and the presence of fusogenic DOPE increases the association with Caco-2 cells, as indicated by flow cytometry analysis (Fig. S5) with the likely consequence of increased membrane binding and subsequent intracellular penetration. In order to extend the toxicity profile of these formulations, the toxicity of the liposomal formulations was also assessed using the Xenopus laevis embryo model. This model can help to bridge the gap between traditional in vitro and preclinical mammalian assays in biomedical research and drug development. Animal models to be employed for organism-based chemical screens have to be small, low-cost and compatible with simple culture conditions to be suitable for highthroughput screening [27]. Xenopus meets these requirements as its fertilization and embryonic development is external and they produce a large number of transparent embryos that are small enough to be placed in 48- or 96-well plates. he cumulative survival of the embryos after 96 h exposure with the liposomes is summarized in Fig. 5. Liposomes containing no 12- bis-THA did not cause any toxicity to the larvae even after incubation at the highest dose (2.65mMlipids). As seen with the eukaryotic cell model, the addition of 12-bis-THA into the liposomes strongly increased the formulation toxicity but no differences were observed between the 12-bis-THA–loaded liposomes and the 12-bis-THA– loaded liposomes with TFDs. Both of these 12-bis-THA–loaded liposomes display toxic potential in this animal model at the specificincubation conditions used (stage 38 to 45) above 5.6 μM12-bis-THA (0.16mMlipids), a value in the same range as the IC50 values obtained for Caco-2 cell line (Table 4) confirming a good correlation between the eukaryotic and the Xenopus laevis model. The dynamics of the different liposome toxicity and the morphology of the surviving embryos (at stage 45) are reported as Supporting Information (Fig. S6). Representative images show that the surviving embryos had no pattern of malformation or any visible phenotype related to toxicity (oedema, lack of pigmentation, bent spine, etc.) [48]. In summary these biological data indicate that the liposomal formulations retain antimicrobial activity and maintain a favourable in vitro activity-to-toxicity ratio (therapeutic index) [49] whilst improving the pharmaceutical properties of the nanoplexes.

CONCLUSIONS

Innovative approaches are needed to curtail antimicrobial resistance. TFDs are being developed as oligonucleotide antimicrobials to combat antibiotic resistance and a nanostructured formulation with 12-bis-THA has been shown to be efficacious in several models. In order to improve their stability,we have created liposomal formulations by decorating the surface of POPC and POPC/DOPE liposomes

with 12-bis-THA, and exploited its ability to complex oligonucleotides to load a model TFD onto the lipid scaffolds. Confocal microscopy imaging was used to assess the ability of liposomes containing fluorescently labelled TFDs to transfect E. coli cells. In the case of the POPC formulations, images evidenced an interaction of liposomes with the bacterial membrane areas richer in cardiolipin, reinforcing the role of this negative lipid in the targeting for 12-bis-THA, like other cationic antimicrobials, towards bacteria. However only POPC/DOPE liposomes effectively delivered the TFD to the E. coli cytoplasm, evidencing the requirement of a fusogenic helper lipid to successfully cross the bacterial membrane and boost transfection. POPC/DOPE liposomes therefore appear extremely promising as vector for the delivery of this new generation of antibacterial drugs. Preliminary biological assays demonstrated a nonnegligible cytotoxic effect of 12-bis-THA towards human Caco-2 cells:future work will focus on the reduction of cytotoxicity by modulating the concentration of 12-bis-THA through its partial replacement with more biocompatible cationic lipids.

MATERIALS AND METHODS

POPC (1-palmitoyl-2-oleoyl-sn-glycero-3-phosphocholine) and DOPE (1,2-dioleoyl-sn-glycero-3-phosphoethanolamine) were purchased from Avanti PolarLipids (Alabaster, AL). 12-bis-THA (1,1′-(dodecane-1,12-diyl)-bis-(9-amino-1,2,3,4-tetrahydroacridinium) (chloride or iodide) was synthesized by Shanghai ChemPartner Co. Ltd. Ultrapurewaterwas obtained bymeans of aMillipore Elix® 3 water purification system.

The oligonucleotide TFDs used in this work were manufactured and purified through HPLC at AxoLabs (Kulmbach, Germany). The TFD used for structural studies has been described elsewhere [15]; it consists of 77 base pairs containing the binding site for the sigma factors of RNA polymerase SigH. The fluorescently labeled Alexa488-Fur TFD was used in imaging and biological assays and contained the binding site for E. coli Fur transcription factor. Its sequence was: 5′-Alexa488-TEGCGATAG AAG TGG ATT TTT CCA CTT CTA* T*C*G-3′, where TEG is a tetraethyl glycol linker and the last nucleotides followed by an asterisk contain a phosphorothioate backbone.

To prepare 12-bis-THA/TFD nanoplexes in water, 500 μL of a waterstock solution of 12-bis-THA at a concentration of 0.23 mg/mL was mixed with 490 μL H2O and vortexed for 30 s. Then, 10 μL of TFD aqueous solution (1 mg/mL) was added, and vortexed for 30 s more. The nanoplexes thereby obtainedwere characterized by a positive-to-negative charge ratio Z+/−=11. To prepare particles in saline solutions, 500 μL of a water stock solution of 12-bis-THA at a concentration of 0.23 mg/mL was mixed with 390 μL H2O and vortexed for 30 s. Then, 10 μL of TFD aqueous solution (1 mg/mL) was added, and vortexed for 30 s more. Finally, 100 μL of 1.5 mol/L solutions of sodium chloride (NaCl) and sodium citrate (Na3Cit) was added to the particle solution.

The lipids POPC and DOPE were weighed in order to obtain a POPC:DOPE = 7:3 weight ratio, in such a way as to obtain a final total concentration of 5mg/mL lipids in the liposomal suspensions. The lipids were firstly dissolved and thoroughly mixed in chloroform or chloroform/methanol. The solvent was evaporated using a gentle N2 flow, and the lipid films were further dried by vacuum pumping for at least 8h.The filmswere hydratedwithwater orwith a TFD solution, depending on the particular protocol, and themixturewas vortexed to obtain a suspension of multilamellar vesicles. In a typical sample, the lipids-to-12-bis-THA mole ratio would be 20:1, while the mole ratio between the bolaamphiphile and the oligonucleotide would be 860:1 (which affords Z+/− = 11), unless specified differently. In order to obtain liposomes, the mixture underwent ten freeze-and thaw cycles (from liquid nitrogen to a 50 °C water bath), unless the oligonucleotide was already present. Eventually, the suspension was extruded ten times through a polycarbonate filter (pore size = 100

nm). If 12-bis-THA was not in the initial dry film, it would be incorporated in the liposomes by a surface decoration method as follows: the bolaamphiphile was dissolved in methanol, then a dry film was obtained by evaporating the solvent under N2, and the appropriate amount of liposomal dispersion was poured on top of the dry film. The sample was vortexed and then kept in orbital stirring for approximately 10 h.

The concentration of 12-bis-THA in the liposomes was ascertained by HPLC analysis, using a Zorbax Eclipse XDB-C18 column (150 × 4.6 mm, 5 μm). The chromatography was carried out at a flow rate 1 mL/min in isocratic conditions, where the mobile phase was KH2PO4 (20 mM)/acetonitrile/triethylamine (60:40:0.5 v/v/v) at pH = 3.8. UV-detection of 12-bis-THA was performed at λ = 254 nm.

The TFD concentration in liposomeswas assessed using the Quant-iT™ OliGreen® fluorescent DNA staining dye (Life Technologies). A fluorescence intensity vs. TFD concentration standard curve was realized by recording the emission spectra of OliGreen® on a LS50B spectrofluorimeter (Perkin-Elmer, Italy); the spectra were acquired in the corrected mode, with an excitation wavelength of 480 nm and 10 nm slits, and the intensity at the emission maximum (520 nm) was plotted against [TFD]. Liposomal sampleswere diluted appropriately to fit in thelinear range. The amount of TFD encapsulated in the liposomes was estimated by measuring the fluorescence of the OliGreen dye before and after the disruption of liposomes with 1 wt.% Triton X-100. DSC analysis was performed with a Q2000 DSC, TA Instruments (New Castle, USA). Roughly 30 mg of each sample was placed in aluminium hermetic pans and analyzed scanning the temperature between 0 °C and 50 °C at 5 °C/min.

DLS analysis was used to infer the size and polydispersity of 12-bis- THA/TFD nanoplexes and of liposomes. For the nanoplexes, a Malvern ZetaSizer ZSwas used, having a red laser (λ=630nm) and the detector placed at 173°. For the liposomes, the instrument used was a Brookhaven BI9000-AT digital autocorrelator, equipped with a green laser (λ = 532 nm; Torus, mpc3000, LaserQuantum, UK) and an APD detector placed at 90°. In both cases, the hydrodynamic diameters were calculated by cumulant analysis of the autocorrelation functions to extract the diffusion coefficients of the dispersed particles, which were then converted into sizes by assuming a spherical shape via the Stokes-Einstein equation.

ζ-potentials were obtained from phase analysis light scattering (PALS) analysis, performed on a Brookhaven ZetaPALS instrument, equipped with a laser operating at 659 nm. The scattered intensity was collected at 15° to determine the electrophoretic mobility; the ζ-potentials were then calculated through the Helmholtz–Smoluchowski equation.

SAXS analysis ofmultilamellar vesicleswas carried outwith a Kratky camera system(HECUS). The incident beamwas a CuKα radiation (λ=1.542 Å) produced by a sealed-tube generator (Seifert ID-303) operating at 1.5 kW; the CuKβ radiation was removed thanks to a 10 μm thick Ni filter. The detector (OED 50 M) contained 1024 channels of width 54 μm, and the sample-to-detector distance was 274 mm. The available Q-range was 0.01–0.55 Å. All measurements were performed at 25 °C (temperature controlled by a Peltier element, accuracy ±0.1 °C); the samples were inserted in either a quartz Mark capillary (1.5mmdiameter) or a paste sample holder, depending on their viscosity, and the cells were kept under vacuum during the experiment. SAXS analysis of liposomes was conducted at the Austrian SAXS beamline (Elettra Synchrotron, Trieste, Italy). The samples were placed in quartz Mark capillaries of 1mmthickness, enclosed in a steel cell; the same capillary was used for the blank to subtract to each sample. Scattering patterns were recorded at room temperature, on a Mar300-image-plate detector (MarResearch, Norderstedt, Germany), by irradiating the samples with an x-ray beam at an 8 keV energy. Irradiation times were in the order of 30 s, and for each sample 3 spectra were acquired and averaged. The sample-to-detector distance of 1308 mm allowed to access a

0.0067–0.46 Å−1 Q-range. Data reduction and background subtraction were performed with the software IGOR Pro (Wavemetrics, Inc.) [24]. Curves obtained with the Kratky camera were iteratively desmeared using the procedure reported by Lake [25]. Data modelling was carried out with the software GAP, provided by Prof. Georg Pabst (Graz University, Austria) [26].

E. coli strain DH5α was grown to mid-log growth (Optical Density 0.2–0.3 at 630 nm) in LB broth. Fresh culture was mixed with an equal volume of liposomes loaded with an Alexa-Fluor488-labelled TFD (λex488/em519) and incubated at room temperature for a total of 1.5 h, under constant agitation in the dark. For the last 30 min, the bacterial membrane was labelled with the fluorescent membrane dye WGATMR (λ ex555/em580 nm, Life Technologies, UK) at a final concentration of 10 μg/mL. The samples were smeared onto poly-L-lysine coated slides (Sigma-Aldrich, UK) and incubated for a further 1 h in the dark at room temperature. Slides were then gently washed with filteredsterilized PBS and dried in the air. Microscopy slides were kept in the dark at 4 °C prior to analysis by confocal microscopy using either a Leica TCS SP5 confocalmicroscope or a Leica TCS SP2, using a 63×oil immersion objective or a 63× water immersion objective, respectively. In both cases, the images were acquired with 488 nm Argon laser excitation (λ em498/ex530 nm) for Alexa488-labeled TFD and with DPSS 561 nmlaser excitation (λ em571/ex620 nm) forWGA-TMR dye labelling the bacterial membrane.

The antibacterial activity of 12-bis-THA–containing formulations was tested against Escherichia coli DH5α using standard procedures, where changes in the optical density (630 nm) after overnight growth is interpreted as bacterial growth inhibition. Bacteria were incubated with liposomes in a concentration range between 5.3 × 10−4 and 5.3 × 10−7 mol/L for the lipids (corresponding to 18–0.018 μmol/L for 12-bis-THA and 1–0.001 μg/mL for TFDs).

Caco-2 cells were grown to 70–80% confluency in 96 well plates, then exposed to liposomes in a concentration range of lipids between 2.65 × 10−3 and 1 × 10−5 mol/L (corresponding to 90 μmol/L and 0.34 μmol/L of 12-bis-THA and 5 to 0.02 μg/mL of TFDs) in serum-free culture medium. After 24 h the formulation was removed and the cell viability examined by measuring the mitochondrial reduction of MTT using A570nm.

All experiments were performed in compliance with the relevant laws and institutional guidelines at the University of East Anglia. The research has been approved by the local ethical review committee according to UK Home Office regulations. Xenopus laevis embryos were obtained as previously described [27]. X. laevis embryos at stage 38 were exposed to liposomes ±12-bis-THA and TFD at concentrations ranging from 2.65 × 10−3 to 4 × 10−5 mol/L of lipids, corresponding to 90 μmol/L and 1.36 μmol/L of 12-bis-THA and 5 to 0.08 μg/mL of TFDs. Embryos were incubated at 18 °C until they reached stage 45.

ACKNOWLEDGEMENTS

This work was funded under the 7-People Framework – Marie Curie Industry and Academia Partnerships & Pathways scheme (grant agreement nr. 612338). We gratefully acknowledge technical assistance from: Mrs. Ghislaine Frébourg (Cryo-TEM; Institut de Biologie Paris-Seine, Université Pierre et Marie Curie, Paris, France); Dr. Paolo Tempesti (in-house SAXS; CSGI and Department of Chemistry,University of Florence, Italy); Dr. Heinz Amenitsch (synchrotron SAXS; Elettra, Trieste, Italy). The authors thank Prof. Alessio Mengoni (Department of Biology, University of Florence, Italy) for providing E. coli for CLSMimaging; Prof. Georg Pabst (University of Graz, Austria) for providing the GAP software free of charge; Dr. Alejandro Marin-Menendez and Dr.Gladys Ruiz Estrada for collaboration in some of the experiments.

REFERENCES

[1] A. Harms, E. Maisonneuve, K. Gerdes, Mechanisms of bacterial persistence during stress and antibiotic exposure, Science 354 (2016) aaf4268, http://dx.doi.org/10.1126/science.aaf4268.
[2] R.R. Watkins, R.A. Bonomo, Overview: global and local impact of antibiotic resistance, Infect. Dis. Clin. N. Am. 30 (2016) 313–322, http://dx.doi.org/10.1016/j.idc.2016.02.001.
[3] A.J. Alanis, Resistance to antibiotics: are we in the post-antibiotic era? Arch. Med. Res. 36 (2005) 697–705, http://dx.doi.org/10.1016/j.arcmed.2005.06.009.
[4] World Health Organization, Antimicrobial Resistance: Global Report on Surveillance, Geneva, Switzerland, 2014.
[5] L. Czaplewski, R. Bax, M. Clokie, M. Dawson, H. Fairhead, V.A. Fischetti, S. Foster, B.F. Gilmore, R.E.W. Hancock, D. Harper, I.R. Henderson, K. Hilpert, B.V. Jones, A. Kadioglu, D. Knowles, S. Ólafsdóttir, D. Payne, S. Projan, S. Shaunak, J. Silverman, C.M. Thomas, T.J. Trust, P.Warn, J.H. Rex, Alternatives to antibiotics—a pipeline portfolio review, Lancet Infect. Dis. 16 (2016) 239–251, http://dx.doi.org/10.1016/S1473-3099(15)00466-1.
[6] M.L. Mangoni, A.M. McDermott, M. Zasloff, Antimicrobial peptides and wound healing: biological and therapeutic considerations, Exp. Dermatol. 25 (2016) 167–173, http://dx.doi.org/10.1111/exd.12929.
[7] K. Braun, A. Pochert, M. Lindén, M. Davoudi, A. Schmidtchen, R. Nordström, M. Malmsten, Membrane interactions of mesoporous silica nanoparticles as carriers of antimicrobial peptides, J. Colloid Interface Sci. 475 (2016) 161–170, http://dx.doi.org/10.1016/j.jcis.2016.05.002.
[8] M. Kutateladze, R. Adamia, Bacteriophages as potential new therapeutics to replace or supplement antibiotics, Trends Biotechnol. 28 (2010) 591–595, http://dx.doi.org/10.1016/j.tibtech.2010.08.001.
[9] A. Extance, Biologics target bad bugs, Nat. Rev. Drug Discov. 9 (2010) 177–178, http://dx.doi.org/10.1038/nrd3129.
[10] T.K. Lind, P. Zielińska, H.P.Wacklin, Z. Urbańczyk-Lipkowska, M. Cárdenas, Continuous flow atomic force microscopy imaging reveals fluidity and time-dependent interactions of antimicrobial dendrimer with model lipid membranes, ACS Nano 8 (2014) 396–408, http://dx.doi.org/10.1021/nn404530z.
[11] B.L. Geller, Antibacterial antisense, Curr. Opin. Mol. Ther. 7 (2005) 109–113 (PMID: 15844617).
[12] M. McArthur, Transcription factor decoys for the treatment and prevention of infections caused by bacteria including clostridium difficile. US Patent App. 13/802,103, 2013.
[13] M. McArthur, M.J. Bibb, Manipulating and understanding antibiotic production in Streptomyces coelicolor A3(2) with decoy oligonucleotides, Proc. Natl. Acad. Sci. 105 (2008) 1020–1025, http://dx.doi.org/10.1073/pnas.0710724105.
[14] V. Weissig, J. Lasch, G. Erdos, H.W. Meyer, T.C. Rowe, J. Hughes, DQAsomes: a novel potential drug and gene delivery system made from Dequalinium™, Pharm. Res. 15 (1998) 334–337, http://dx.doi.org/10.1023/A:1011991307631.
[15] M. Mamusa, C. Resta, F. Barbero, D. Carta, D. Codoni, K. Hatzixanthis,M.McArthur, D. Berti, Interaction between a cationic bolaamphiphile and DNA: the route towards nanovectors for oligonucleotide antimicrobials, Colloids Surf. B Biointerfaces 143

(2016) 139–147, http://dx.doi.org/10.1016/j.colsurfb.2016.03.031.
[16] J. Lasch, A. Meye, H. Taubert, R. Koelsch, J. Mansa-ard, V. Weissig, Dequalinium TM vesicles form stable complexes with plasmid DNA which are protected from DNase attack, Biol. Chem. 380 (1999)http://dx.doi.org/10.1515/BC.1999.080.
[17] A. Marín-Menéndez, C.Montis, T. Díaz-Calvo, D. Carta, K. Hatzixanthis, C.J.Morris,M. McArthur, D. Berti, Antimicrobial nanoplexes meet model bacterial membranes: the key role of Cardiolipin, Sci Rep 7 (2017) 41242, http://dx.doi.org/10.1038/srep41242.
[18] B.S. Pattni, V.V. Chupin, V.P. Torchilin, New developments in liposomal drug delivery, Chem. Rev. 115 (2015) 10938–10966, http://dx.doi.org/10.1021/acs.chemrev.5b00046.
[19] D.A. Balazs, W. Godbey, Liposomes for use in gene delivery, J. Drug Deliv. 2011 (2011) 1–12, http://dx.doi.org/10.1155/2011/326497.
[20] Z. Drulis-Kawa, A. Dorotkiewicz-Jach, Liposomes as delivery systems for antibiotics, Int. J. Pharm. 387 (2010) 187–198, http://dx.doi.org/10.1016/j.ijpharm.2009.11.033.
[21] P. Fillion, A. Desjardins, K. Sayasith, J. Lagacé, Encapsulation of DNA in negatively charged liposomes and inhibition of bacterial gene expression with fluid liposome-encapsulated antisense oligonucleotides, Biochim. Biophys. Acta Biomembr. 1515 (2001) 44–54, http://dx.doi.org/10.1016/S0005-2736(01)00392-3.
[22] D. Lichtenberg, Characterization of the solubilization of lipid bilayers by surfactants, Biochim. Biophys. Acta Biomembr. 821 (1985) 470–478, http://dx.doi.org/10.1016/0005-2736(85)90052-5.
[23] P. Luciani, D. Berti, M. Fortini, P. Baglioni, C. Ghelardini, A. Pacini, D. Manetti, F. Gualtieri, A. Bartolini, L. Di Cesare Mannelli, Receptor-independent modulation of reconstituted Gαi protein mediated by liposomes, Mol. BioSyst. 5 (2009) 356, http://dx.doi.org/10.1039/b815042g.
[24] S.R. Kline, Reduction and analysis of SANS and USANS data using IGOR Pro, J. Appl. Crystallogr. 39 (2006) 895–900, http://dx.doi.org/10.1107/S0021889806035059.
[25] J.A. Lake, An iterative method of slit-correcting small angle X-ray data, Acta Crystallogr. 23 (1967) 191–194, http://dx.doi.org/10.1107/S0365110X67002440.
[26] G. Pabst, Global properties of biomimetic membranes: perspectives on molecular features, Biophys. Rev. Lett. 01 (2006) 57–84, http://dx.doi.org/10.1142/S1793048006000069.
[27] C.A. Webster, D. Di Silvio, A. Devarajan, P. Bigini, E. Micotti, C. Giudice, M. Salmona, G.N.Wheeler, V. Sherwood, F.B. Bombelli, An early developmental vertebrate model for nanomaterial safety: bridging cell-based and mammalian toxicity assessment, Nanomedicine 11 (2016) 643–656, http://dx.doi.org/10.2217/nnm.15.219.
[28] J.N. Israelachvili, Intermolecular and Surface Forces, 3. ed. Elsevier, Acad. Press, 2011.
[29] H. Farhood, N. Serbina, L. Huang, The role of dioleoyl phosphatidylethanolamine in cationic liposome mediated gene transfer, Biochim. Biophys. Acta Biomembr. 1235 (1995) 289–295, http://dx.doi.org/10.1016/0005-2736(95)80016-9.
[30] D. Nicolosi, M. Scalia, V.M. Nicolosi, R. Pignatello, Encapsulation in fusogenic liposomes broadens the spectrum of action of vancomycin against Gram-negative bacteria, Int. J. Antimicrob. Agents 35 (2010) 553–558, http://dx.doi.org/10.1016/j.ijantimicag.2010.01.015.
[31] I. Koltover, An inverted hexagonal phase of cationic liposome-DNA complexes related to DNA release and delivery, Science 281 (1998) 78–81, http://dx.doi.org/10.

1126/science.281.5373.78.
[32] R. Zhang, R.M. Suter, J.F. Nagle, Theory of the structure factor of lipid bilayers, Phys. Rev. E 50 (1994) 5047–5060, http://dx.doi.org/10.1103/PhysRevE.50.5047.
[33] G. Pabst, J. Katsaras, V.A. Raghunathan, M. Rappolt, Structure and interactions in the anomalous swelling regime of phospholipid bilayers †, Langmuir 19 (2003) 1716–1722, http://dx.doi.org/10.1021/la026052e.
[34] J.F. Nagle, S. Tristram-Nagle, Structure of lipid bilayers, Biochim. Biophys. Acta Rev. Biomembr. 1469 (2000) 159–195, http://dx.doi.org/10.1016/S0304-4157(00)00016-2.
[35] G. Pabst, M. Rappolt, H. Amenitsch, P. Laggner, Structural information from multilamellar liposomes at full hydration: full q -range fitting with high quality xray data, Phys. Rev. E 62 (2000) 4000–4009, http://dx.doi.org/10.1103/PhysRevE.62.4000.
[36] G. Pabst, R. Koschuch, B. Pozo-Navas, M. Rappolt, K. Lohner, P. Laggner, Structural analysis of weakly ordered membrane stacks, J. Appl. Crystallogr. 36 (2003) 1378–1388, http://dx.doi.org/10.1107/S0021889803017527.
[37] K. Sakai, H. Tomizawa, K. Tsuchiya, N. Ishida, H. Sakai, M. Abe, Characterizing the structural transition of cationic DPPC liposomes from the approach of TEM, SAXS and AFM measurements, Colloids Surf. B: Biointerfaces 67 (2008) 73–78, http://dx.doi.org/10.1016/j.colsurfb.2008.07.017.
[38] N. Kučerka, M.-P. Nieh, J. Katsaras, Small-angle scattering from homogenous and heterogeneous lipid bilayers, Adv. Planar Lipid Bilayers Liposomes, Elsevier, 2010.
[39] L.D. Renner, D.B.Weibel, Cardiolipin microdomains localize to negatively curved regions of Escherichia coli membranes, Proc. Natl. Acad. Sci. 108 (2011) 6264–6269, http://dx.doi.org/10.1073/pnas.1015757108.
[40] R.H. Houtkooper, F.M. Vaz, Cardiolipin, the heart of mitochondrial metabolism, Cell. Mol. Life Sci. 65 (2008) 2493–2506, http://dx.doi.org/10.1007/s00018-008-8030-5.
[41] V.Weissig, C. Lizano, V.P. Torchilin, Selective DNA release fromDQAsome/DNA complexes at mitochondria-like membranes, Drug Deliv. 7 (2000) 1–5, http://dx.doi.org/10.1080/107175400266722.
[42] L. Lombardi, M.I. Stellato, R. Oliva, A. Falanga, M. Galdiero, L. Petraccone, G. D'Errico, A. De Santis, S. Galdiero, P. Del Vecchio, Antimicrobial peptides at work: interaction of myxinidin and its mutant WMR with lipid bilayers mimicking the P. aeruginosa and E. coli membranes, Sci Rep 7 (2017) 44425, http://dx.doi.org/10.1038/srep44425.
[43] S. Morein, A.-S. Andersson, L. Rilfors, G. Lindblom, Wild-type Escherichia coli cells regulate the membrane lipid composition in a “window” between gel and non-lamellar structures, J. Biol. Chem. 271 (1996) 6801–6809, http://dx.doi.org/10.1074/jbc.271.12.6801.
[44] M. Rappolt, A. Hickel, F. Bringezu, K. Lohner,Mechanism of the lamellar/inverse hexagonal phase transition examined by high resolution X-ray diffraction, Biophys. J. 84 (2003) 3111–3122, http://dx.doi.org/10.1016/S0006-3495(03)70036-8.
45] M.J. Weiss, J.R. Wong, C.S. Ha, R. Bleday, R.R. Salem, G.D. Steele Jr., L.B. Chen, Dequalinium, a topical antimicrobial agent, displays anticarcinoma activity based on selective mitochondrial accumulation, Proc. Natl. Acad. Sci. 84 (1987) 5444–5448.
[46] X.-L.Wang, T. Nguyen, D. Gillespie, R. Jensen, Z.-R. Lu, A multifunctional and reversibly polymerizable carrier for efficient siRNA delivery, Biomaterials 29 (2008)

15–22, http://dx.doi.org/10.1016/j.biomaterials.2007.08.048.
[47] P. Reynier, D. Briane, R. Coudert, G. Fadda, N. Bouchemal, P. Bissieres, E. Taillandier, A. Cao, Modifications in the head group and in the spacer of cholesterol-based cationic lipids promote transfection in melanoma B16-F10 cells and tumours, J. Drug Target. 12 (2004) 25–38, http://dx.doi.org/10.1080/10611860410001683040.
[48] G.N. Wheeler, K.J. Liu, Xenopus : an ideal system for chemical genetics, Genesis 50 (2012) 207–218, http://dx.doi.org/10.1002/dvg.22009.
[49] A.J. Trevor, B.G. Katzung, S.B. Masters, M. Kruidering-Hall, Pharmacology Examination & Board Review, McGraw-Hill Medical, New York, 2010.

SCHEMES

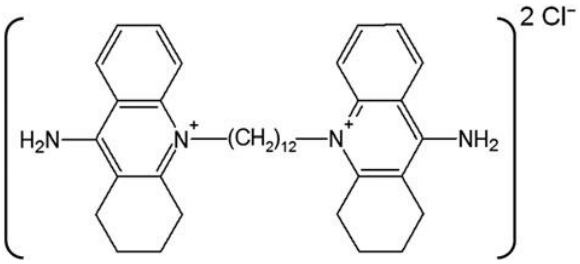

Scheme 1. Molecular structure of 12-bis-THA.

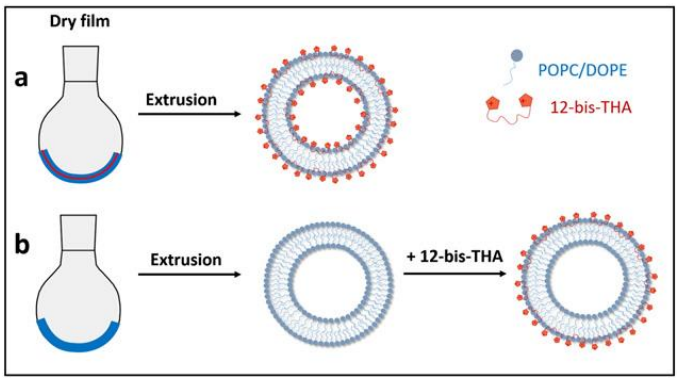

Scheme 2. Pictorial representation of the two protocols employed for liposome preparation. a) “Co-extrusion” method: lipids and 12-bis-THA are both present in the initial dry film; b) “Surface decoration” method: only lipids are present in the initial dry film; 12-bis-THA is added to liposomes after extrusion.

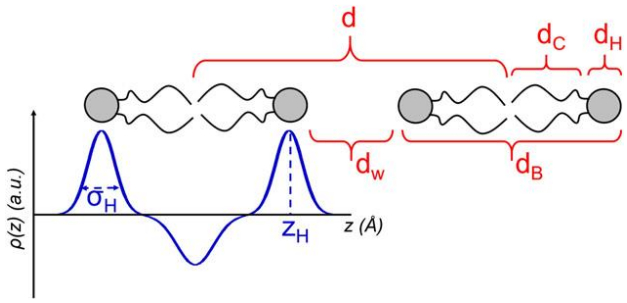

Scheme 3. Pictorial representation of amodel lipid bilayer and the corresponding electron density profile, where: d = lamellar spacing; dW (Å): thickness of water layer between headgroups (MLV only); dB (Å): bilayer thickness; dH (Å): headgroup thickness; dC (Å): half thickness of hydrophobic region; zH (Å) and σH (Å): center and width, respectively, of the Gaussians representing the headgroups.

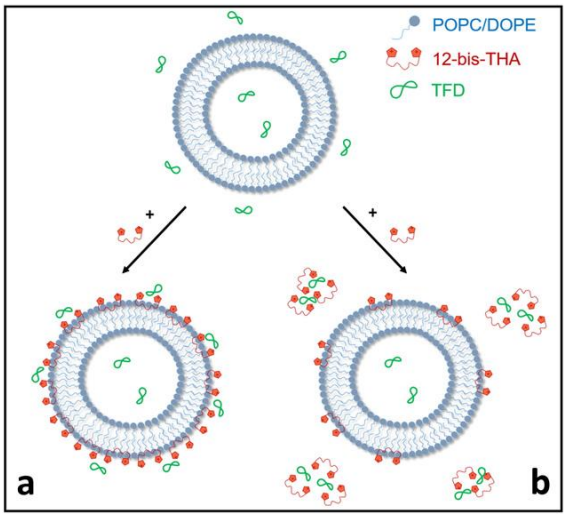

Scheme 4. Schematic illustration of possible scenarios unfolding upon addition of 12-bis-THA to POPC/DOPE liposomes in a TFD solution. (a) 12-bis-THA adsorbs onto the lipid bilayer and attracts the TFD by electrostatic interaction. (b) 12-bis-THA preferentially forms isolated nanoplexes with the TFD in the bulk solution.

FIGURES

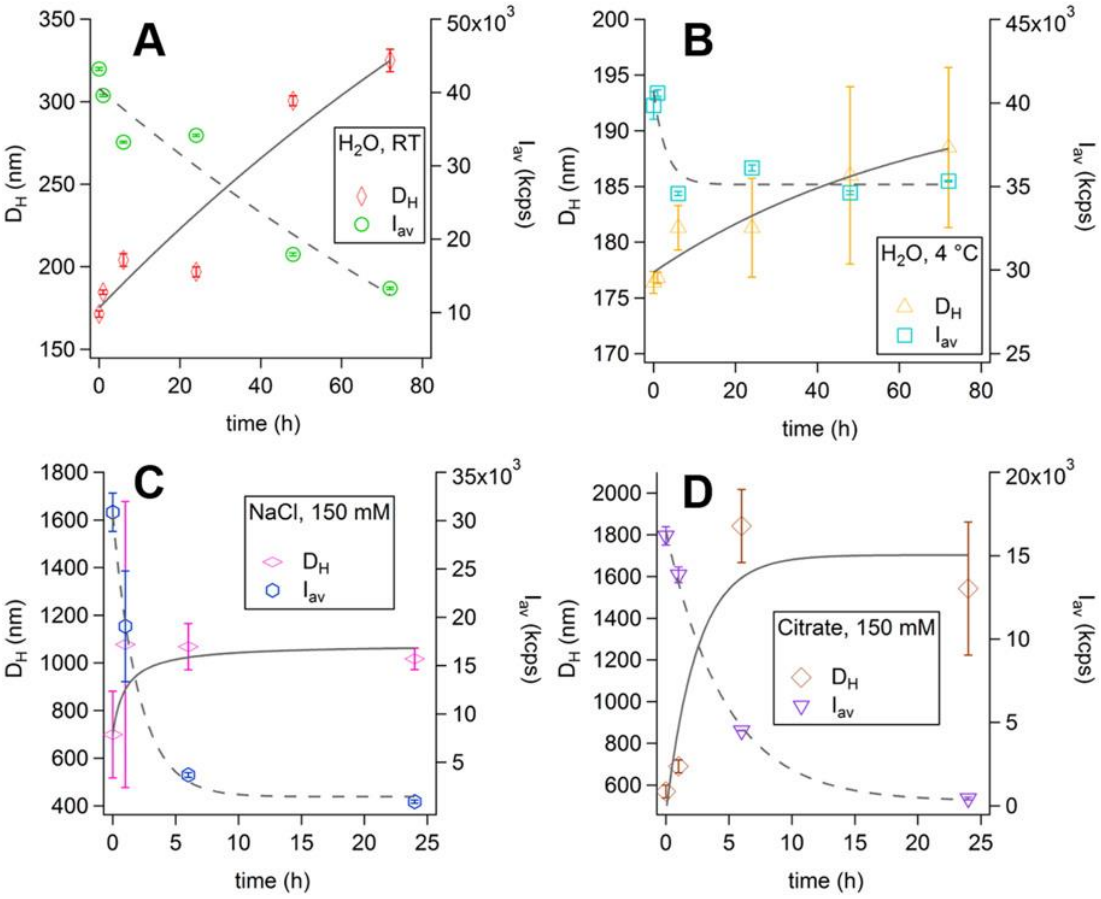

Fig. 1. Colloidal stability of 12-bis-THA/TFD polyplexes in differentmedia: (A)water, 4 °C; (B)water, RT; (C) NaCl 150mM, RT; (D) sodiumcitrate 150mM, RT. Sampleswere analysed by light scattering analysis. DH (nm) = hydrodynamic diameter; Iav (kcps)= average scattering intensity. Lines are not data fits but a guide for the eye. Data shown are mean ± standard deviation.

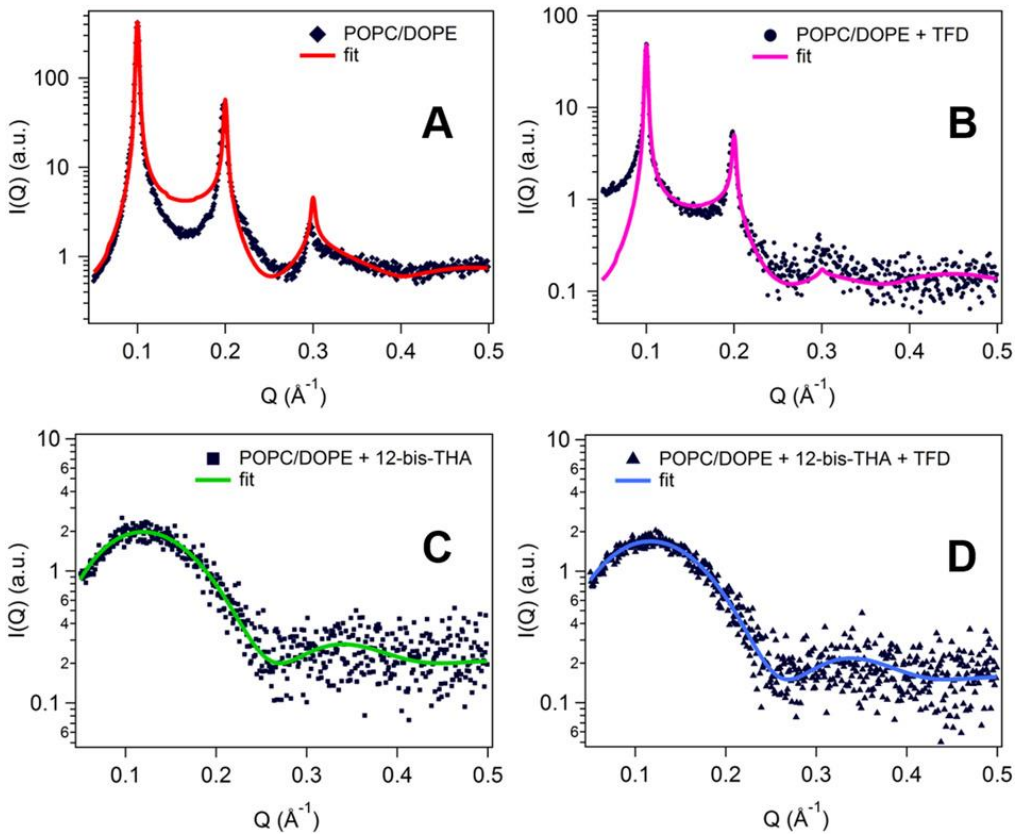

Fig. 2. SAXS patterns of POPC/DOPE bilayers: (A) neat; (B) with TFD; (C) with 12-bis-THA (20:1 mole ratio); (D) with 12-bis-THA and TFD (Z+/－=22).

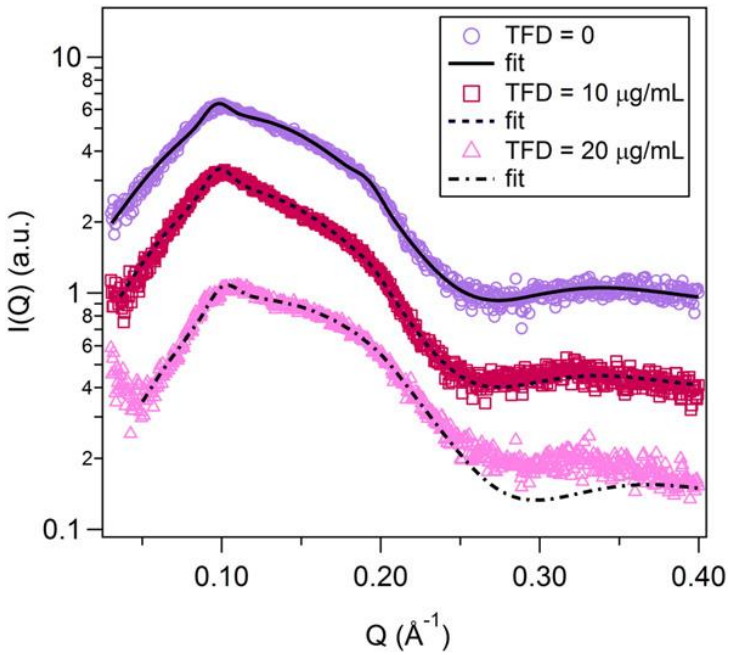

Fig. 3. SAXS patterns obtained for POPC/DOPE/12-bis-THA liposomes containing growing concentrations of TFD. Experimental data are represented with markers, while model curves are represented by lines.

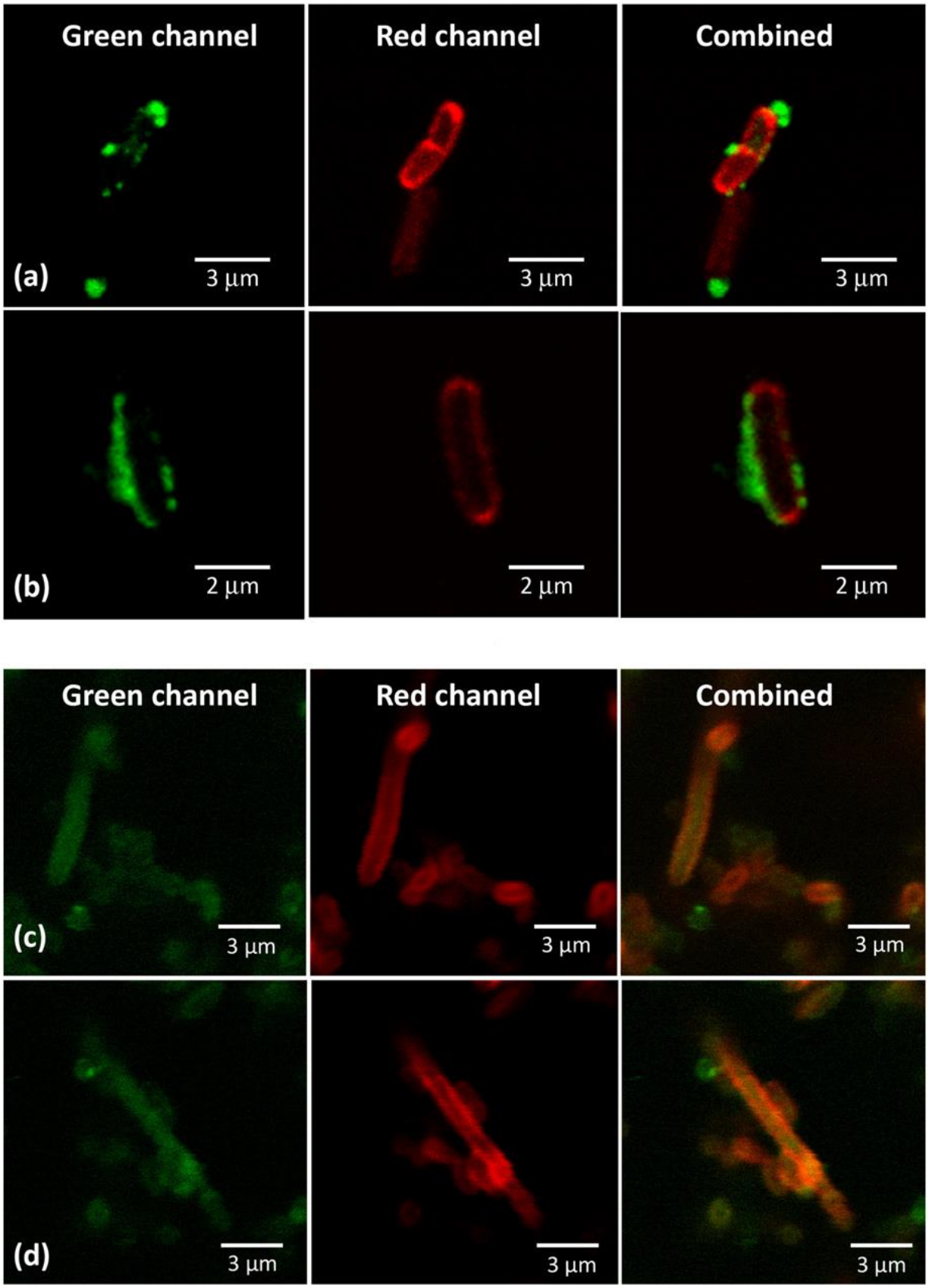

Fig. 4. Confocal microscopy images of the interaction between liposomes loaded with a fluorescent TFD (green) and E. coli bacteria (red). Separate channels and combined channels displayed. (a) and (b) POPC/12-bis-THA/TFD liposomes; (c) and (d) POPC/DOPE/12-bis-THA/TFD liposomes.

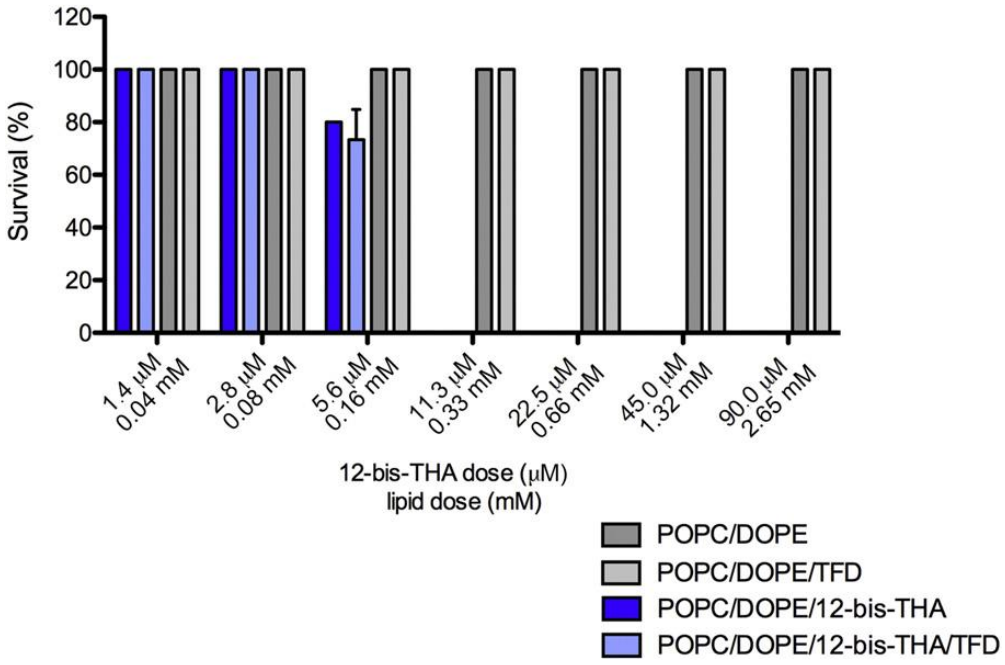

Fig. 5. Xenopus laevis nanotoxicity assay. Xenopus laevis larvae survival after exposure to different liposome formulations from stage 38 to stage 45 at 18 °C. Histograms shown are of 30 embryos at each concentration. Date are mean ± S.D.

TABLES

Composition		DH (nm)	PDI	ζ-Pot (mV)
POPC		109 ± 1	0.07	−23 ± 2
POPC +12-bis-THA	Co-extruded	105 ± 2	0.09	+20 ± 3
(20:1 mol ratio)	Decoration	120 ± 2	0.1	+16 ± 1
POPC/DOPE		111 ± 2	0.04	−16 ± 4
(POPC/DOPE) + 12-bis-THA (20:1 mol ratio)	Co-extruded	115 ± 4	0.04	+20 ± 1
	Decoration	124 ± 2	0.16	+28 ± 2

Table 1 Physical-chemical characterization of liposomes (lipids: 5mg/mL, with POPC:DOPE=70:30wt.%) without and with 12-bis-THA, incorporated via two different protocols. Hydrodynamic diameters (DH, nm) and size polydispersity (PDI) obtained by cumulant analysis of the DLS autocorrelation functions; ζ-potentials (ζ-Pot,mV) obtained by PALS analysis of the same samples. Data are mean ± standard deviation.

Parameter	a	b	c	d
d (Å)	62.82 (±0.01)	62.75 (±0.01)	N/A	N/A
zH (Å)	19.4 (±0.2)	20 (±0.1)	17.5 (±0.1)	17.6 (±0.1)
σH (Å)	3 *	3 *	3 *	3 *
Ndiff	0	0	1	1
N. of lamellae	25	26	N/A	N/A
dB (Å)	51	52	47	47
dW (Å)	12	11	N/A	N/A

Table 2 Results of SAXS data modelling (Fig. 2) and calculation of some structural properties. D (Å): lamellar spacing; zH (Å) and σH (Å): center and width, respectively, of the Gaussians representing the headgroups; Ndiff: ratio of non-interacting bilayers (i.e. ULVs); N. of lamellae: average number of interacting lamellae; dB (Å): bilayer thickness; dW (Å): thickness of inter-lamellar water space. N/A = not applicable; * = constrained parameter.

Parameter	[TFD] 0 µg/mL	[TFD] 10 µg/mL	[TFD] 20 µg/mL
d (Å)	64.9	64.3	62
zH (Å)	17.79	18.4	15.93
σH (Å)	2.996	3.2	3
Ndiff	0.972	0.9638	0.969
N. of lamellae	2	2 *	2 *
dB (Å)	48	50	N/A

Table 3 Results of SAXS datamodelling of the samples of Fig. 3 with GAP software and calculation of some structural properties. d (Å): lamellar spacing; zH (Å) and σH (Å): center and width, respectively, of the Gaussians representing the headgroups; Ndiff: ratio of uninteracting bilayers (i.e. ULVs); N. of lamellae: average number of interacting lamellae; dB (Å): bilayer thickness. * = constrained parameter.

Samples	12-bis-THA MIC (µmol/L)	12-bis-THA IC50 (µmol/L)
POPC/DOPE	–	ND
POPC/DOPE/TFD	–	ND
POPC/DOPE/12-bis-THA/TFD	1.1	33.9 (±1.4)
POPC/DOPE/12-bis-THA	1.1	31.8 (±3.1)

Table 4 Biological evaluation of liposomes in antibacterial activity (MIC) against E. coli and cytotoxicity (IC50) in Caco-2 cells after 24 h exposure. ND: no observable toxicity at concentrations tested. Data are mean ± standard deviations.